Rates and Equilibria for a Photoisomerizable Antagonist at the Acetylcholine Receptor of *Electrophorus* Electroplaques

MAURI E. KROUSE, HENRY A. LESTER, NORBERT H. WASSERMANN, and BERNARD F. ERLANGER

From the Division of Biology, California Institute of Technology, Pasadena, California 91125; and the Department of Microbiology, Columbia University Cancer Center/Institute of Cancer Research, New York 10032

ABSTRACT Voltage-jump and light-flash experiments have been performed on isolated *Electrophorus* electroplaques exposed simultaneously to nicotinic agonists and to the photoisomerizable compound 2,2′-bis-[α-(trimethylammonium)methyl]-azobenzene (2BQ). Dose-response curves are shifted to the right in a nearly parallel fashion by 2BQ, which suggests competitive antagonism; dose-ratio analyses show apparent dissociation constants of 0.3 and 1 μM for the *cis* and *trans* isomers, respectively. Flash-induced *trans* → *cis* concentration jumps produce the expected decrease in agonist-induced conductance; the time constant is several tens of milliseconds. From the concentration dependence of these rates, we conclude that the association and dissociation rate constants for the *cis*-2BQ-receptor binding are $\sim 10^8$ M^{-1} s^{-1} and 60 s^{-1} at 20°C; the Q_{10} is 3. Flash-induced *cis* → *trans* photoisomerizations produce molecular rearrangements of the ligand-receptor complex, but the resulting relaxations probably reflect the kinetics of buffered diffusion rather than of the interaction between *trans*-2BQ and the receptor. Antagonists seem to bind about an order of magnitude more slowly than agonists at nicotinic receptors.

INTRODUCTION

According to present concepts of competitive antagonism at nicotinic receptors, *d*-tubocurarine and related drugs interact directly with the agonist site; this occupation prevents the binding of agonists and the resulting activation of the channel. Most electrophysiological studies suggest that the antagonist-receptor interaction is characterized by a single dissociation constant of $\sim 10^{-7}$ M, although more recent binding studies reveal two separate binding reactions whose association constants flank this value (Neubig and Cohen, 1979; Sine and Taylor,

Address reprint requests to Dr. Henry A. Lester, Division of Biology 156-29, California Institute of Technology, Pasadena, CA 91125. Dr. Krouse's present address is Dept. of Physiology, John Curtin School for Medical Research, Australian National University, Canberra ACT 2601, Australia.

J. GEN. PHYSIOL. © The Rockefeller University Press · 0022-1295/85/08/0235/22$1.00

Volume 86 August 1985 235–256

1981). This paper is concerned with the kinetics of the antagonist-receptor interaction.

Hill (1909) first studied the response to a sudden change of tubocurarine concentration in the solution bathing a frog muscle. Although he hoped to determine the molecular rates of the antagonist-receptor interaction, the measurements were limited by the drug's diffusion into the muscle rather than by the molecular rates of interest. del Castillo and Katz (1957) measured the responses to brief iontophoretic pulses of both antagonist and agonist from twin pipettes onto the same synapse. In their experiments, tubocurarine's inhibitory effect decayed over several seconds, much more slowly than expected from the diffusion of tubocurarine in solution. It was suggested that this slow recovery represented the molecular rate of dissociation of the tubocurarine-receptor complex. Less direct experiments have since suggested much faster rates (Blackman et al., 1975; Sheridan and Lester, 1977; Colquhoun et al., 1979), and it has been shown that the iontophoresis experiment was distorted by the phenomenon of buffered diffusion within the synaptic cleft: tubocurarine's macroscopic rate of action is at least an order of magnitude slower than its molecular binding rates because its rate of diffusion is slowed by high-affinity binding to its receptors (Armstrong and Lester, 1979).

Other relaxation techniques have been of limited use for kinetic data on the antagonist-receptor interaction. The binding is not thought to be voltage-sensitive, so that voltage jumps couple only indirectly to this interaction and are instead dominated by the voltage-dependent processes of (*a*) channel gating and (*b*) open channel blockade by the antagonist (Manalis, 1977; Colquhoun et al., 1979). Single channel measurements would be complicated by (*a*) multiple closed states of the receptor and (*b*) channel gating produced by the antagonists themselves (Trautmann, 1982; Morris et al., 1983); this activation might not involve the same binding mechanisms as the competitive antagonism.

The light-flash technique (Lester and Chang, 1977; Lester and Nerbonne, 1982) does enable the experimenter to jump the concentration of ligand within the synaptic cleft. Although the prototypical competitive antagonist *d*-tubocurarine is not photosensitive, 2,2′-bis-[α-(trimethylammonium)methyl]azobenzene (2BQ) (Fig. 1) is photoisomerizable and displays competitive antagonism. The apparent dissociation constant is similar to that for *d*-tubocurarine (Lester et al., 1980). The present study was therefore undertaken to measure directly the rate constants for the antagonist-receptor interaction. The data have already been presented briefly in abstract form (Krouse et al., 1982, 1984) and as part of a Ph.D. dissertation (Krouse, 1984).

METHODS

Reagents

trans-2BQ was synthesized as described (Wassermann and Erlanger, 1981). The pure *cis* isomer was obtained by exposing a nearly saturated solution (2 mM) to ultraviolet (UV) light, followed by high-performance liquid chromatography (Nerbonne et al., 1983). Tetrodotoxin and the agonists (acetylcholine, carbachol, and suberyldicholine) were purchased from Sigma Chemical Co., St. Louis, MO.

Electrophysiology

In a typical experiment, 5–11 applications of agonist and numerous washes were completed on a single isolated electroplaque in an apparatus similar to that described by Sheridan and Lester (1977). Two preliminary agonist applications were performed to check the reproducibility of the agonist-induced currents and to provide a measure of the time of diffusion of agonist molecules from pool A (the solution bathing the innervated face) to receptors. During subsequent agonist applications, voltage-jump episodes were recorded after the estimated diffusion time had elapsed. After each agonist application, the solution in pool A was exchanged for Ringer three times over a period of 5 min. At the end of the wash cycles, agonist-induced currents had disappeared. For measurements of agonist-induced currents in the presence of 2BQ, pool A was preincubated with 2BQ alone for

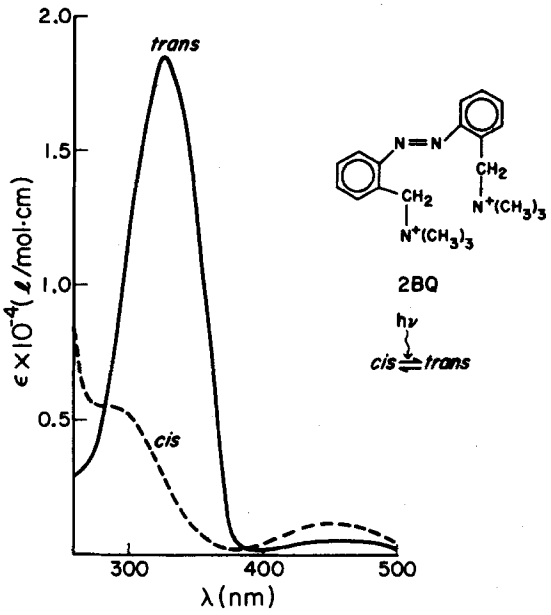

FIGURE 1. Structure of 2BQ and optical absorption spectra of the *cis* and *trans* isomers. The absorption maximum of the *trans* isomer is at 327 nm ($\epsilon = 1.9 \times 10^4$ l/mol·cm); an isosbestic point is observed at 287 nm ($\epsilon = 0.54 \times 10^4$ l/mol·cm).

5–10 min. After trials in agonist and 2BQ, pool A was washed several times with Ringer over 15 min. All experiments in the presence of 2BQ were preceded and followed by trials with agonist alone. Agonist-induced currents were measured by subtraction of the passive membrane responses; as detailed in previous publications, these passive responses could be isolated either in trials without agonist or, in the presence of agonist, by evoking voltage jumps in a region of membrane potential where the agonist-induced conductance is negligible (Sheridan and Lester, 1977).

Rate constants were measured for the relaxations in response to both voltage jumps and light flashes. Voltage-jump relaxations could usually be described with a single exponential, using a least-squares fit to the semilogarithmic plot of the approach to steady state (Figs. 9 and 10). Some voltage-jump relaxations, and most light-flash relaxations, required two exponentials; these were fit by the method of least squares.

Photochemistry

The thermal *cis-trans* isomerization of 2BQ in solution is negligibly slow at or below room temperature. The two isomers interconvert in the presence of light; the mole fraction of each isomer in a solution depends on the wavelength of irradiation. This mole fraction is determined from the optical spectra of the solutions by linear interpolation between the A_{327}/A_{281} ratios for the pure isomers (cf. Fig. 1). These concepts are used to measure the potency of a given flash for *trans* → *cis* and *cis* → *trans* photoisomerization (Nass et al., 1978; Lester and Nerbonne, 1982; Sheridan and Lester, 1982). Table I presents the photoisomerization potencies for the filters and flashes used with 2BQ in the experiments. We often employed a predominantly *trans* or *cis* photostationary solution (TPSS or CPSS, respectively), obtained by prolonged irradiation either with unfiltered flashes (TPSS, 80% *trans*) or with a 365-nm lamp (CPSS, 85% *cis*).

The optical arrangement was similar to that previously described (Nass et al., 1978). There were two improvements: (*a*) the xenon short-arc flash tube was placed at one focus of a polished ellipsoidal mirror rather than in a standard lamp housing; and (*b*) the energy storage bank had a capacitance of 2,100 μF and was charged to 450 V. The flash intensity rose to a peak in <100 μs and fell with a time constant of 500 μs. This arrangement

TABLE I

Photoisomerization Potencies for 2BQ with the Filters Used

Filter	λ (± Half-width at half-maximum)	Isomerization potency	
		k_c	k_t
	nm	*flash*$^{-1}$	
341 interference	341±10	0.02	0.18
UG11 (UV)	328±47	0.09	0.51
UG1 (UV)	362±33	0.23	0.55
BG3 (blue)	400±55	0.60	0.40
No filter	300–800	2.40	0.60
OG550 (orange)	>550	<0.01	<0.01

yielded a fivefold increase in the UV light intensity at the preparation, as compared with the previous apparatus (Nass et al., 1978).

Light from the flash-lamp was filtered to remove λ < 290 nm (WG 295, Schott Optical Glass, Inc., Duryea, PA) and focused on the preparation with a quartz lens (focal length, 75 mm; numerical aperture, 0.16) (Nargeot et al., 1982). Filters were placed in the light path between the ellipsoidal mirror and the focusing lens.

A few experiments required briefer flashes; these were delivered at 440 nm with the flash-lamp–pumped dye laser described by Sheridan and Lester (1982).

Simulations

Numerical simulations of the relaxations were performed with the TUTSIM program (Applied i, Palo Alto, CA), which integrates linear differential equations.

RESULTS

Equilibrium Measurements

In *Electrophorus* electroplaques, steady state agonist-induced conductances are conveniently measured during hyperpolarizing voltage jumps (Sheridan and

Lester, 1975, 1977). Our experiments employed the three agonists suberyldicholine (Fig. 2), carbachol, and acetylcholine. Results with agonist alone generally agreed with previous studies showing that steady state conductances increase with increasing agonist concentration and with more negative membrane potential (Adams, 1975; Neher and Sakmann, 1975; Sheridan and Lester, 1975, 1977). 2BQ induces no detectable conductance by itself, but it does block agonist-induced conductances.

Dose-ratio studies were performed in order to characterize the 2BQ-receptor interaction. In such experiments, one measures steady state conductances at several agonist concentrations in the presence of varying concentrations of 2BQ, and from these data abbreviated log-dose response curves are constructed (Fig. 3). Concentrations were selected to give agonist-induced conductances between

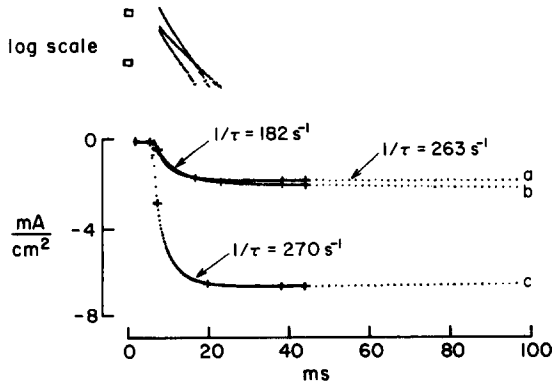

FIGURE 2. Superimposed agonist-induced currents from three different voltage-clamp trials during a dose-ratio experiment with 2BQ and suberyldicholine at 6°C. Passive and capacitive currents have been subtracted. In each episode, the voltage was stepped from +60 to −150 mV 4 ms after the start. The agonist-induced current approached a new steady state value along an approximately exponential time course (semilog plots are shown at the top; the boxes define a 10-fold range of current). Trace *a*: 10 μM suberyldicholine plus 2 μM 2BQ (*trans*-photostationary state); *b*: 3 μM suberyldicholine; *c*: 10 μM suberyldicholine. See text for a discussion of the rate constants. Experiment 427T39.

30 and 60% of the maximal response. The measure of interest is the ratio of agonist concentrations giving equal steady state conductance levels in the presence and absence of 2BQ. With 2BQ at concentrations of ≤4.0 μM, dose-response curves were shifted to higher agonist concentrations with no change in slope, and 2BQ did not decrease the maximum agonist-induced current at high agonist concentrations (Krouse, 1984). Under these conditions, 2BQ therefore behaves as a competitive antagonist. At concentrations of >4 μM, 2BQ did exert noncompetitive blockade; this action is discussed more fully below.

From the dependence of the dose ratio on 2BQ concentration, one obtains an apparent dissociation constant K_i of 0.7 μM for the *trans*-photostationary state (Fig. 4). As found previously for *d*-tubocurarine (Lester et al., 1975), this value was the same for all voltages in the range tested (−60 to −150 mV), which implies

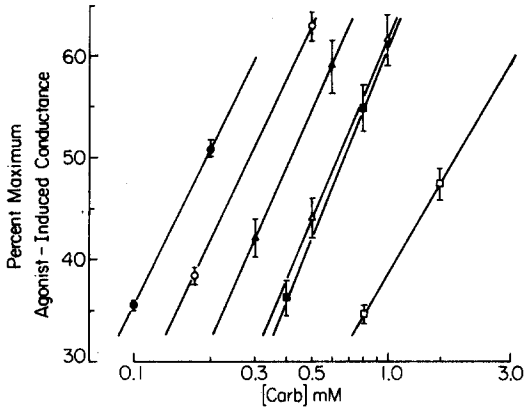

FIGURE 3. Abbreviated dose-response plots, showing inhibition of agonist-induced currents by 2BQ. Data are from voltage-clamp trials like those of Fig. 2. Agonist, carbachol; antagonist, 2BQ (*trans*-photostationary state). Voltage, −120 mV; 20°C. Means ± SEM from measurements on four cells. TPSS-2BQ concentrations: ●, 0.0 μM; ○, 1.0 μM; ▲, 2.0 μM; △, 3.0 μM; ■, 4.0 μM; □, 6.0 μM.

that the apparent affinity of 2BQ for the receptor is voltage-independent. It should be noted that the assumptions of the dose-ratio method may be inappropriate for nicotinic acetylcholine receptors. The Discussion contains a more detailed evaluation of the shape of the dose-ratio plot.

The most interesting result of the dose-ratio studies was of course the variation in inhibition with the isomeric composition of the 2BQ solution. One would expect the apparent affinity constant $1/K_i$ to depend linearly on the mole fraction

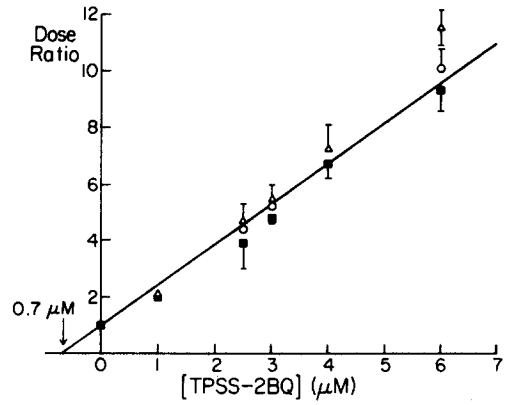

FIGURE 4. Dose-ratio analysis of experiments like those of Figs. 2 and 3. The line is a weighted least-squares fit to all the data at 2BQ concentrations of ≤4 μM, constrained to pass through the point (0, 1). The data for individual voltages give slopes differing by <5%. The intercept on the concentration axis gives the apparent dissociation constant (K_i = 0.7 μM). ■, −70 mV; ○, −100 mV; △, −130 mV. See text for further information.

of each isomer; therefore, it is more revealing to plot this parameter than K_i (Fig. 5). The pure *cis* isomer has an equilibrium binding constant of 0.33 μM for the receptor; the pure *trans* isomer binds one-third as strongly.

Kinetic Measurements: Voltage-Jump Relaxations

Although the voltage-jump experiments described above were designed primarily to give information about equilibrium binding properties, they also gave preliminary kinetic information. In the experiment of Fig. 2, for instance, the presence of 2BQ caused a reduction of agonist-induced conductance, but there was little or no change in the rate constant of the voltage-jump relaxation. This suggests that the blockade re-equilibrates more slowly than the time scale of the voltage-jump relaxation. We therefore expected that more direct experiments, based on flash-induced concentration jumps of 2BQ, would reveal a distinct component

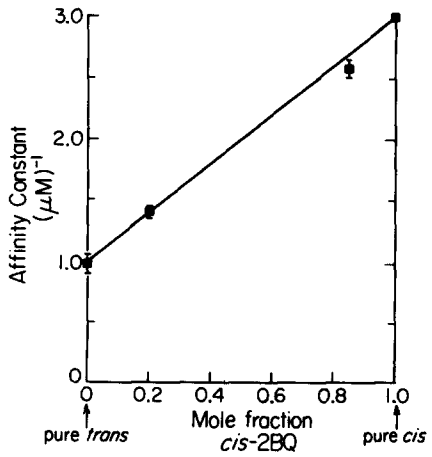

FIGURE 5. Isomeric dependence of the affinity constant, from data like those of Figs. 2–4. Each point represents the mean ± SEM of measurements on four different cells.

caused by the 2BQ-receptor interaction on a time scale slower than the agonist-receptor interaction. This expectation was confirmed.

Concentration-Jump Relaxations

UV FLASHES In solutions containing mostly *trans*-2BQ, UV light increases the mole fraction of *cis* in solution. This "antagonist concentration jump" leads to a net decrease in the conductance and provides the clearest data on the kinetics of the interaction between *cis*-2BQ and the receptor.

The typical UV-flash relaxation (Fig. 6) consists of two components. The faster component, termed $1_{t\text{-}f}$, is either a delay (period of zero slope) or a small increase in agonist-induced current; it is best seen under different conditions and will therefore be described later. The slower component, $2_{t\text{-}f}$, is the decrease in agonist-induced current expected to accompany an increase in the antagonist concentration. The point of greatest interest is that this decrease occurred on a

time scale roughly one order of magnitude slower than the voltage-jump relaxations thought to reflect primarily the agonist-receptor interaction.

Our experiments were guided by the idea that component $2_{l\text{-}f}$ is dominated by the molecular kinetics of the interaction between *cis*-2BQ and the nicotinic receptor. Several detailed models are presented in the Discussion; for present purposes, we employ the simple equation

$$\textit{cis}\text{-2BQ} + \mathrm{R} \underset{k_-}{\overset{k_+}{\rightleftharpoons}} \textit{cis}\text{-2BQ}\cdot\mathrm{R}. \qquad (1)$$

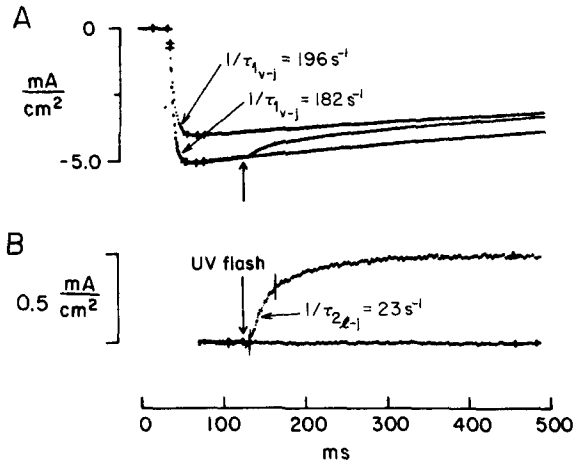

FIGURE 6. A UV-flash relaxation during a voltage-clamp trial. At the start of the trial, 2BQ is present in the *trans*-photostationary state (2 μM); the agonist is carbachol (500 μM). The trial consists of three episodes at intervals of 3 s. Panel *A* shows agonist-induced currents; passive and capacitive currents have been subtracted. 50 ms after the start of each episode, the voltage was jumped from +60 to −150 mV. As in the experiment of Fig. 2, the agonist-induced current approached a new steady state value along an approximately exponential time course. The rate constants for these voltage-jump relaxations are 150–200 s^{-1}. Because the time scale is five times longer than that of Fig. 2, the traces also show a slow decrease in agonist-induced current, presumably caused by open channel block by 2BQ (see text). The flash was delivered at the arrow in the second episode, jumping the *cis*-2BQ concentration from 0.4 to 0.98 μM. After an initial delay of a few milliseconds (see text), the conductance decreased with a rate constant of ~25 s^{-1}. Panel *B* presents the difference between traces 2 and 3 at higher gain to show the UV-flash relaxation. Temperature, 6°C. Experiment 1122T24.

For Scheme 1, the relaxation rate constant for component $2_{l\text{-}f}$ is expected to equal the sum $k_- + fk_+[\textit{cis}\text{-2BQ}]$. The dissociation rate constant k_- would dominate at low 2BQ concentrations; at higher concentrations, the relaxation rate constant would be determined by the forward binding rate $fk_+[\textit{cis}\text{-2BQ}]$. The factor f, which is between 0 and 1, decreases with agonist concentration and reflects the more rapidly equilibrating occupancy of binding sites by the agonist;

this occupancy effectively reduces the probability of forming the *cis*-2BQ-receptor complex. The most important evidence for the view that Scheme 1 dominates the kinetics is the behavior of component 2_{l-f} as a function of drug concentration (Fig. 7). As expected, (*a*) $1/\tau$ for component 2_{l-f} increases with 2BQ concentration, and (*b*) this increase is less steep with increased agonist concentration.

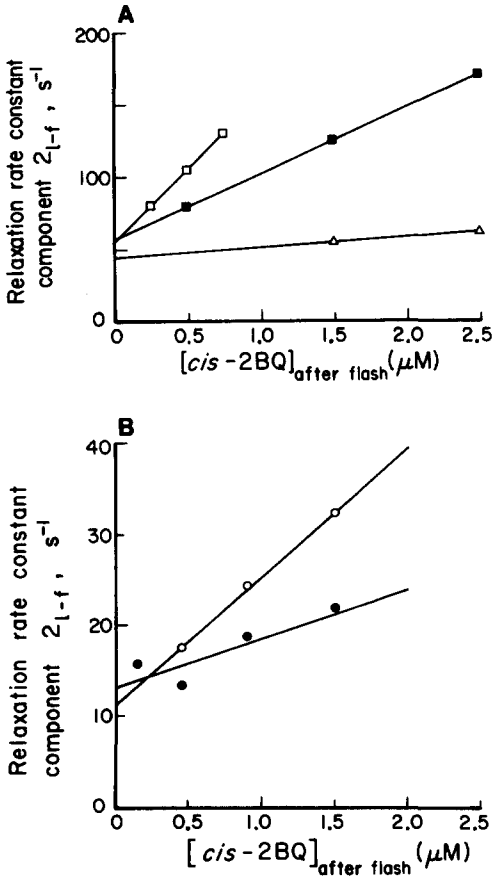

FIGURE 7. Relaxation rate constants vs. [*cis*-2BQ]. Data are from experiments like that of Fig. 6, at various concentrations of 2BQ and carbachol. The lines are least-squares fits to the data. (*A*) 6°C. Data at 150 (□) and 250 (■) μM carbachol are from the same cell. Δ, 400 μM carbachol. (*B*) 20°C. ○, 150 μM carbachol; ●, 400 μM.

The data of Fig. 7 thus allow preliminary estimates of the rate constants for association and dissociation of *cis*-2BQ. From the zero-concentration intercepts, one obtains dissociation rate constants k_- of 10.7 ± 0.8 s^{-1} (mean ± SD, 6 cells) at 6°C and 60.4 ± 13.9 s^{-1} (17 cells) at 20°C. These intercepts did not change with voltage over the range −90 to −150 mV. From the slope of the steepest line at each temperature, one can conclude that the forward binding rates are at

least 2×10^7 M^{-1} s^{-1} at 6°C and at least 7×10^7 M^{-1} s^{-1} at 20°C. The Discussion contains a more complete treatment of the factor f, allowing for better estimates of the forward binding rate constants.

ALTERNATIVE EXPLANATIONS Because our strategy relies so heavily on the interpretation of component 2_{l-f}, it is well to emphasize how the observations rule out alternative explanations. For instance, is component 2_{l-f} dominated by buffered diffusion? The UV flash increases the *cis*-2BQ concentration both within the synaptic cleft and in the external solution. However, the synaptic cleft has such a high receptor concentration that equilibrium inhibition might be established only after *cis*-2BQ molecules diffuse into the cleft from the external solution. This diffusion would be slowed by repeated antagonist binding (Armstrong and Lester, 1979). Two observations argue against buffered diffusion in our experiments. (*a*) Buffering would be reduced by decreasing the number of binding sites for 2BQ (Armstrong and Lester, 1979), for instance by increasing the agonist concentration. However, the relaxation rate constants decreased with increasing agonist concentration (Fig. 7), contrary to the expectations of the buffering model. (*b*) Rather low temperature dependences ($Q_{10} \sim 1.3$) are indicative of buffered diffusion (Armstrong and Lester, 1979), but our most reliable kinetic data—the zero-concentration intercept of plots like those of Fig. 7—show a Q_{10} of ~3 over the range 6–30°C. A Q_{10} of 3 is within the range expected for ligand-protein interactions. Thus, buffered diffusion does not seem to dominate component 2_{l-f}.

Are the relaxations dominated by the interaction of *trans*-2BQ and the receptor? In most of our experiments (e.g., that of Fig. 7), the *cis*-2BQ concentration after a single flash was varied by bathing the cell in varying initial concentrations of TPSS-2BQ. Other experiments were simply conducted at a fixed TPSS-2BQ concentration; relaxations were measured as a series of UV flashes converted the solution to the CPSS (Krouse, 1984). The rate constants increased during the series, contrary to the expectation for a model that is similar to Scheme 1 but in which kinetics are dominated by *trans*-2BQ.

Molecular Rearrangements

In addition to concentration-jump experiments, the light-flash technique makes possible a unique class of experiments in which ligand molecules already bound to receptors are manipulated photochemically to produce a molecular rearrangement of the ligand-receptor complex (Nass et al., 1978; Lester and Nerbonne, 1982). Because of this direct action, such perturbations generally produce more rapid responses than do concentration jumps. The response to a molecular rearrangement does not depend on the direction or amplitude of the bulk concentration changes, although later events may reflect these changes.

We have no direct information about the photoisomerization efficiency of bound 2BQ as opposed to 2BQ in solution. Spectral measurements with a covalently bound azobenzene agonist suggest that such differences are minor (Sheridan and Lester, 1982); however, in the absence of relevant data for 2BQ, we shall describe the amplitudes of these relaxations in a qualitative fashion.

EXPERIMENTS AT THE *CIS*-PHOTOSTATIONARY STATE With predominantly

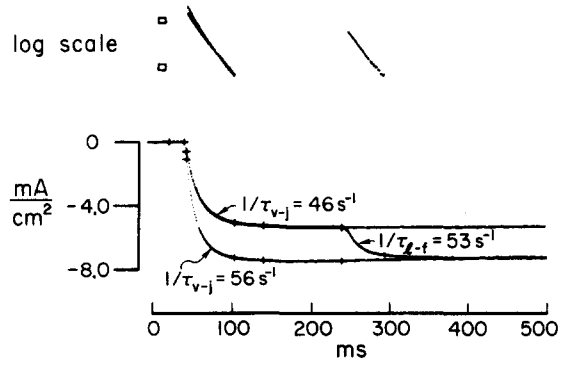

FIGURE 8. Visible-flash relaxations at 6°C and −150 mV in the simultaneous presence of suberyldicholine (3 μM) and 2BQ (1 μM). At the beginning of the trial, the 2BQ was in the *cis*-photostationary state. A visible flash (during the second episode) jumped the *cis*-2BQ concentration from 0.85 to 0.23 μM. The resulting conductance increase is dominated by a rapid relaxation called component 1_{l-f}. Semilog plots are shown at the top; the relaxation rate constants are nearly equal for the voltage-jump and light-flash relaxations. Experiment 682IT80.

cis-2BQ solutions and unfiltered flashes, the molecular rearrangments were expected to arise predominantly from *cis* → *trans* photoisomerizations of bound *cis*-2BQ molecules, because (*a*) this isomer binds more strongly to receptors, (*b*) it was present in higher concentrations, and (*c*) *cis* → *trans* flux predominates in unfiltered flashes (see Table I). We therefore expected that these experiments would reveal the kinetics of the *trans*-2BQ-receptor interaction.

Such flashes did produce increases in the conductance as the newly created *trans*-2BQ molecules left the receptors. When acetylcholine and suberyldicholine were the agonists, the increase occurred with a rate constant that was indistin-

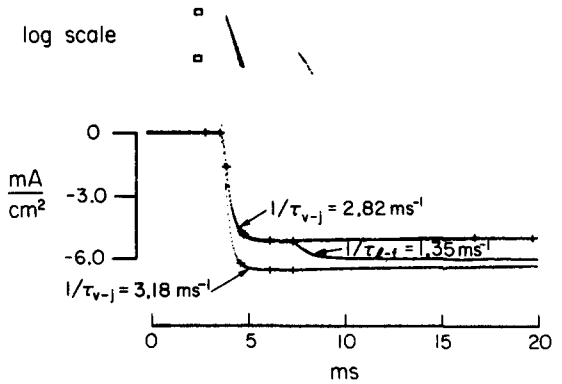

FIGURE 9. Laser-flash relaxations at 20°C in the simultaneous presence of carbachol (200 μM) and 2BQ (1 μM). The protocol is the same as in Fig. 8. The laser flash jumps the *cis*-2BQ concentration from 0.85 to 0.20 μM. Note that the voltage-jump relaxations are faster than the light-flash relaxation. See text. Experiment 617T70.

guishable (±10%) from that of the voltage jump in the next episode (Fig. 8). At temperatures of 20°C or higher with carbachol as the agonist, the agonist-receptor interaction was characterized by rate constants greater than ~2 ms^{-1}. Under these conditions, the flash-lamp discharge could no longer be considered instantaneous on the time scale of the relaxations. Therefore, the light-flash relaxations were evoked with a pulsed laser (Fig. 9). Under these conditions, the light-flash relaxation was clearly slower than the voltage-jump relaxation, which suggests that the dissociation of *trans*-2BQ had become rate-limiting.

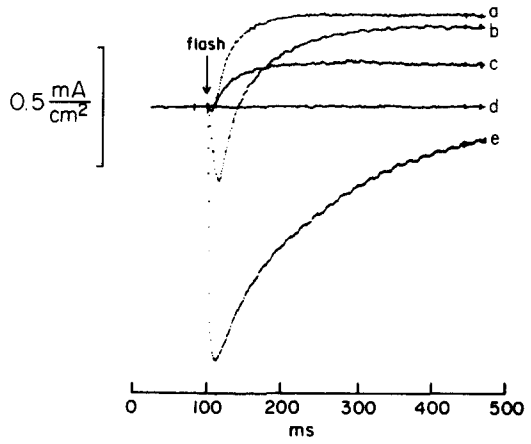

Filter	[*cis*-2BQ] after flash	$1/\tau_2$	Trace
		s^{-1}	
UG11 (UV)	0.98	20	*a*
BG3 (blue)	0.90	10	*b*
341 interference	0.65	18	*c*
OG550 (orange)	0.40	—	*d*
None (visible)	0.40	6.1	*e*

FIGURE 10. Agonist-induced currents from episodes in the simultaneous presence of carbachol (1 mM) and 2BQ (2 μM). At the start of each episode, the 2BQ was in the *trans*-photostationary state ([*cis*-2BQ] = 0.4 μM); the relaxations were superimposed on a steady agonist-induced current of 5.1 mA/cm^2. The flash was filtered differently for each episode. See text and Table I. Voltage, −150 mV; temperature, 6°C. Experiment 1122T64.

EXPERIMENTS AT THE *TRANS*-PHOTOSTATIONARY STATE In cells exposed simultaneously to TPSS-2BQ and to agonist, the kinetics depend strongly on how the flash is filtered (Fig. 10). As the *cis* → *trans* photoisomerization potency increases (cf. Table I), the rapid conductance increase, component 1_{I-f}, is larger. This result is expected because (*a*) roughly half of the inhibition is produced by the 20% of *cis*-2BQ in TPSS-2BQ, and (*b*) a flash converts the bound *cis*-2BQ to *trans*-2BQ. Fig. 11 explains how the subsequent slower conductance decrease,

component 2_{t-f}, is also expected as equilibrium is re-established. An unexpected finding in the experiment of Fig. 10 is that component 2_{t-f} also becomes slower as the *cis* → *trans* photoisomerization potency increases. Although traces *a* and *b* have nearly the same initial and final state, the decrease in trace *b* occurs with a rate constant roughly half as large as that of trace *a*. With unfiltered flashes (trace *e*), the relaxation is slowed even further, to a rate constant less than one-

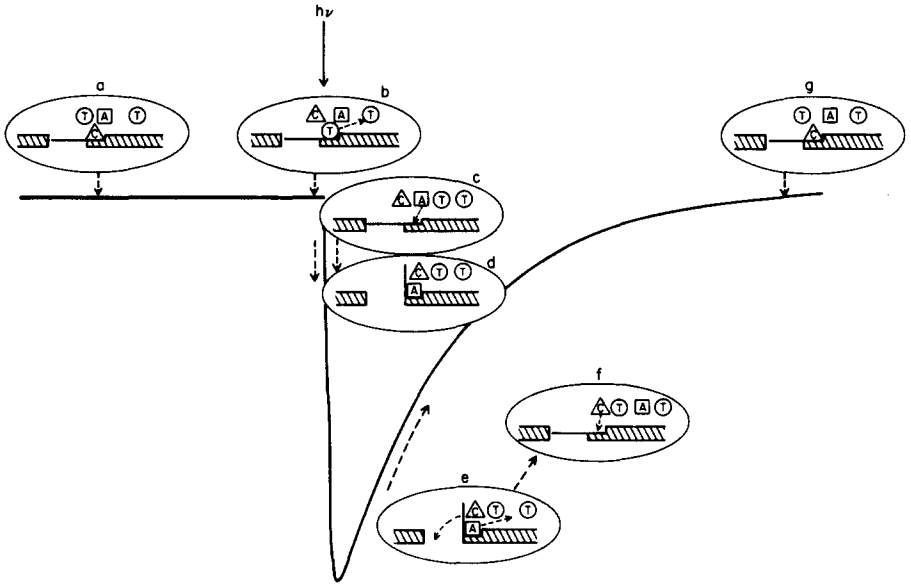

FIGURE 11. Cartoon to explain the relaxation in response to unfiltered flashes with TPSS-2BQ, as in the experiment of Fig. 10, trace *e*. The flash did not change the concentrations of *cis*- and *trans*-2BQ in the solution, but the agonist-induced conductance increased and then decreased back to the initial value. Our simple scheme neglects the complex stoichiometry of channel activation. T, *trans*; C, *cis*; A, agonist. The experiment begins at equilibrium (*a*). A flash leads to photoisomerization of 2BQ molecules. Bound *cis*-2BQ molecules isomerize to *trans*-2BQ, which leave the receptor (*b*), and agonist molecules in solution can then bind to the unoccupied receptor sites (*c*). After the agonist binding, the channels open (*d*), producing the increase in voltage-clamp current associated with component 1. After a normal opening, channels close and agonist molecules dissociate from the receptors (*e*). *cis*-2BQ molecules in solution are free to bind to the vacated sites (*f*), thus preventing agonist binding. This decline in the conductance back to the initial state (*g*) is associated with component 2.

third that of the UV flash. We do not have a full explanation for this slowing; possibilities are presented in the Discussion.

DISCUSSION

This paper completes our investigation of acetylcholine receptors in *Electrophorus* electroplaques with photoisomerizable azobenzene derivatives. Previous studies dealt with agonists and with open channel blockers (Lester and Nerbonne, 1982;

Sheridan and Lester, 1982; Nerbonne et al., 1983); the present data describe inhibition by a competitive antagonist. Like other members of the series, the 2BQ molecule has the important property that the *cis* and *trans* isomers differ in pharmacological potency. We have exploited this property to study the kinetics of the interaction between 2BQ and the receptor; these kinetics have been interpreted in terms of the molecular rate constants for the association and dissociation events.

The experiments are somewhat limited by the fact that the two isomers differ by only a factor of 3 in their apparent affinities for the receptor; therefore, a concentration jump from zero antagonist activity could not be produced. Also, it is not possible to obtain reliable data at either very large or very small concentrations of the agonist or antagonist, because these conditions involve only small changes of the conductance. Nonetheless, it is possible to give a reasonably consistent kinetic and equilibrium description of the interaction between *cis*-2BQ and the receptor.

2BQ as a Competitive Antagonist

The dose-response data, i.e., the parallel shift in the dose-response curves, are consistent with competitive antagonism as the major action of 2BQ under the conditions of our studies (concentrations of ≤ 4 μM and voltages between -60 and -150 mV). As usual with such studies, one needs to exclude the possibility that 2BQ is only a noncompetitive antagonist, with a large excess of "spare receptors." We performed a few experiments to show that maximal responses could in fact be obtained with carbachol even in the presence of 1 μM 2BQ (Krouse, 1984); more complete studies done previously under the same conditions (Sheridan and Lester, 1977; Lester et al., 1978) showed that the test concentrations of carbachol used were indeed high enough to reveal any noncompetitive blockade.

In addition, 2BQ does exhibit a form of noncompetitive antagonism, open channel blockade. However, this complication was not serious, because the rate of blockade was slow under our conditions and this effect could be subtracted from the measured agonist-induced currents. If the local anesthetic effect were significant, light flashes would cause photodissociation of bound 2BQ molecules from their binding sites within channels; this would lead to increases in the current on a submillisecond time scale. Such step increases have been observed with the light-sensitive acetylcholine channel blocker EW-1 (Lester et al., 1979; Krouse, M. E., unpublished observations). However, no such step was observed in our experiments, even at the highest 2BQ concentration (5 μM). It can thus be concluded that the light-flash relaxations were not distorted by the effects of open channel blockade. Experiments like that of Fig. 6 suggest, however, that it would be possible to study this open channel blockade directly by delivering flashes several seconds after a step to a hyperpolarized voltage.

MODELS FOR THE BINDING REACTIONS The equilibrium binding constant K_i for the 2BQ-receptor interaction was calculated from dose-ratio studies. This method was originally formulated for a case where (*a*) the receptor R can be

completely inhibited by the binding of a single antagonist molecule I, and (*b*) agonist molecules A bind noncooperatively (see, for instance, Jenkinson, 1960). However, it is well known that the nicotinic receptor binds two or more agonist molecules per channel; presumably, each agonist site can bind antagonist molecules as well. A more general scheme, then, would be written:

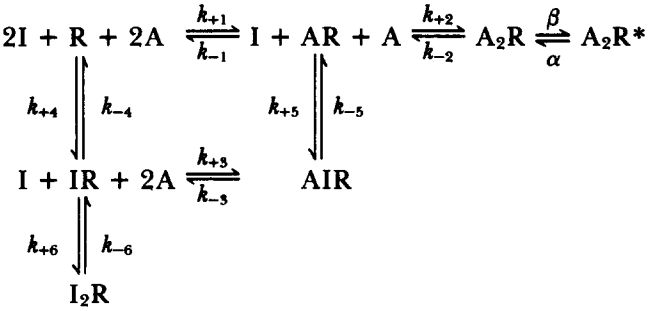

(2)

The A_2R^* state has the open channel. Each of the three possible antagonist binding reactions would influence the experimentally measured inhibition. If all three antagonist binding reactions have the same equilibrium binding constant (K_i), the dose ratio is simply

$$D = 1 + [I]/K_i; \tag{3}$$

i.e., the dose-ratio plots are linear with a slope equal to $1/K_i$.

For other combinations of dissociation constants, the dose-response curves are no longer shifted in a parallel fashion by the antagonist (cf. Krouse, 1984); the complete expression is

$$D = \frac{[A]/K_1(1 + [I]/K_5) + \{([A]/K_1)^2(1 + [I]/K_5)^2 + (2[A]/K_1 + 1)(1 + 2[I]/K_4 + [I]^2/K_4K_6)\}^{1/2}}{2[A]/K_1 + 1}. \tag{4}$$

Even if one confines the measurements to a particular response amplitude, the dose-ratio plots are nonlinear. The plot is upwardly concave (i.e., has a sigmoid start) if the affinity constant increases for the second antagonist ($1/K_6$); the concavity has the opposite sense if the second binding is weaker than the first. However, these nonlinearities decrease as the level of activation increases and they would be quite small for our experimental results, which were taken near the half-maximal response (Colquhoun, 1973). The relationship between antagonist binding sites and the shape of the dose-ratio curve has also been addressed by Pennefather and Quastel (1981). The departures from linearity in our equilibrium data do suggest a slight upward concavity (cf. Fig. 4), so that one would suspect a tighter second binding. This observation does not agree with the suggestion of Sine and Taylor (1981) that there are pre-existing sites of high and low affinity for antagonists on BC3-H1 cells. However, our data are insufficiently precise for a more detailed comparison on this topic. The important point can be summarized as follows: the K_i estimated from the dose-ratio plot is

determined by the smaller of the two equilibrium dissociation constants, K_4 or K_5.

Kinetic Constants for the Interaction Between cis-2BQ and the Receptor

The light-flash relaxations are attributed to the binding and dissociation of 2BQ. We now consider the molecular interpretation for such data in terms of Scheme 2. Fig. 12 shows simulated light-flash relaxations using the protocol of Fig. 6 (a UV flash producing a relaxation from a low to a high level of inhibition). The relaxations are approximately exponential and they are dominated by the antagonist-receptor binding step with the largest rate constants. It can therefore be stated that the relaxation rate constants of Fig. 7 do refer to the faster step;

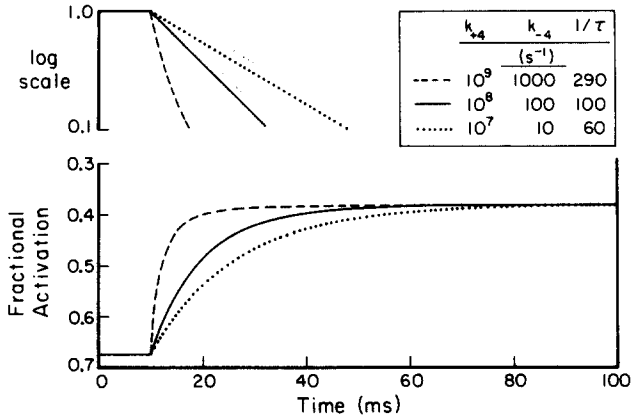

FIGURE 12. Simulated concentration-jump relaxations for a UV flash as in the experiment of Fig. 6. At the time of the flash, the *cis*-2BQ concentration was jumped from 0.2 to 2 μM and the agonist concentration remained constant at 100 μM. The rate constants $k_{\pm}$ differed for each simulation, but the ratio $K_4 = k_{-4}/k_{+4}$ was always 1 μM. The value for k_{-5} and k_{-6} was 100 s^{-1} and the value for k_{+5} and k_{+6} was 10^8 M^{-1} s^{-1}, so that K_5 and K_6 also equaled 1 μM. The value of K_1, K_2, and K_3 was 100 μM, with instantaneous equilibration at the agonist binding sites; α = 3,000 s^{-1}; β = 3×10^4 s^{-1}.

however, the data do not allow for a choice as to which step ($k_{\pm 4}$ or $k_{\pm 5}$) is the faster.

DISSOCIATION RATE The theoretical concentration dependence of these rate constants is shown in Fig. 13*A* for the simplest possible case, i.e., all three antagonist-receptor binding constants are equal. The calculations confirm that the zero-concentration intercept is the rate constant for dissociation of the antagonist-receptor complex. The plots have a sigmoid start, however, so that extrapolations from the linear portion would give underestimates of the true dissociation rate constant. Therefore, the estimated dissociation rate constants for *cis*-2BQ (60 s^{-1} at 20°C and 11 s^{-1} at 6°C) may be too small by 10–20%.

ASSOCIATION RATE The model relaxations also predict the variation in relaxation rate constants with agonist concentration. Here the point of interest

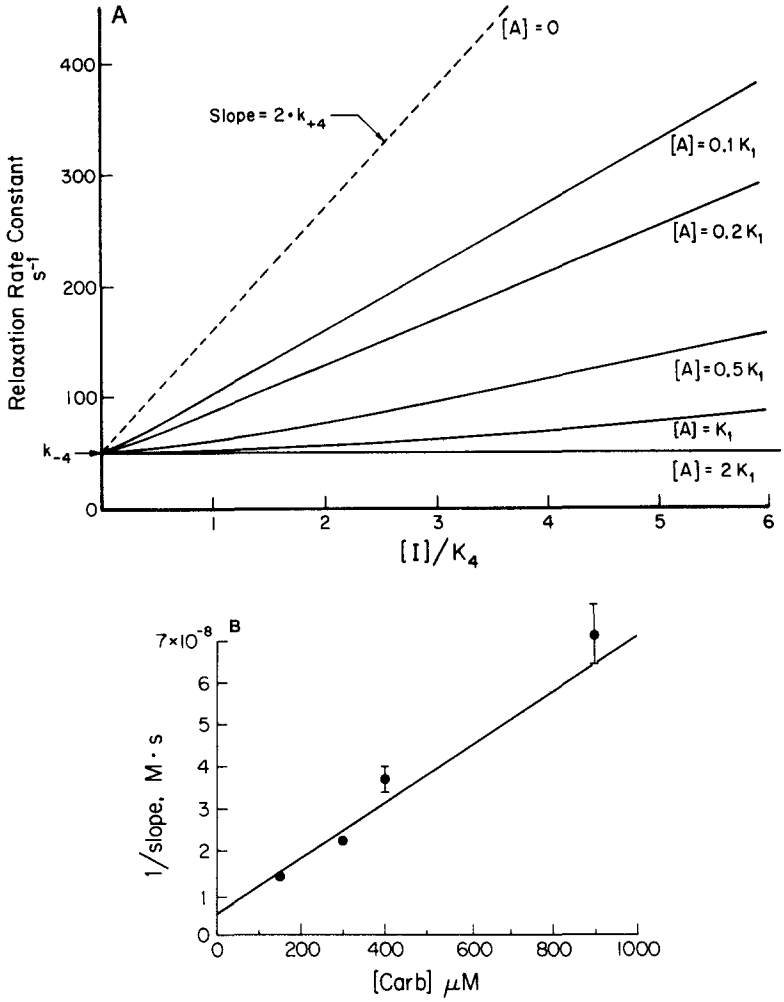

FIGURE 13. (*A*) Calculated relation between drug concentrations and the rate constant of light-flash relaxations. For each agonist concentration, 10 relaxations like those of Fig. 11 were simulated at varying antagonist concentrations [I]. The plots should be compared with the experimental data in Fig. 7. The calculations assume that the three antagonist-receptor interactions have equal rate and equilibrium constants ($k_4 = k_5 = k_6 = 5 \times 10^7$ M^{-1} s^{-1}; $k_{-4} = k_{-5} = k_{-6} = 50$/s). The other assumed parameters equal those of Fig. 11. (*B*) Data are from experiments, including that of Fig. 7*B*, at 20°C on four cells from a single fish. The straight line is a least-squares fit, weighted for the errors at each point; the intercept at zero agonist concentration is 2×10^8 M^{-1} s^{-1}. See text for discussion.

is the factor f, the fractional forward binding rate that results from the rapidly equilibrating occupation of the antagonist binding site by the agonist. The kinetic simulations summarized in Fig. 13 reveal that f can be approximated well by a simple hyperbolic relation, $f = 1/(1 + [A]/K')$, where K' depends on $k_{\pm 1}$, $k_{\pm 2}$, α,

and β. (An explicit formula is not available for K', which does not in general equal the agonist concentration giving a half-maximal response.) Therefore, simple reciprocal plots were used to extrapolate f to unity at zero agonist concentration; an example of such a plot suggests that the largest measured slopes, in experiments like those of Fig. 7, are a factor of 1.5–2 less than the actual forward binding rate constant, $k_{+4} = k_{+5} = k_{+6}$ (Fig. 13*B*). (This estimate includes a correction for the fact that the extrapolated value is actually $1/2k_{+4}$, because we assume two equivalent binding sites.) We conclude that k_{+4} is $\sim 1 \times 10^8$ M^{-1} s^{-1} at 20°C and $\sim 0.2 \times 10^8$ M^{-1} s^{-1} at 6°C.

COMPARISON WITH EQUILIBRIUM MEASUREMENTS With these estimates of the binding rate constants for *cis*-2BQ, we can calculate the ratio k_-/k_+ to obtain an equilibrium value of 0.6 μM. This estimate should be considered correct only to within a factor of 3 because of (*a*) uncertainties about the actual molecular model, (*b*) errors in the extrapolation to zero agonist concentration, and (*c*) scatter in the data themselves. Therefore, the calculated equilibrium value, based on the kinetic measurements, certainly shows satisfactory agreement with the equilibrium measurements ($K_i = 0.3$ μM).

Rates of Drug-Receptor Binding

The present data encourage us to make a few general comments about the rate constants for ligand bindings at the nicotinic acetylcholine receptor. These rates have been investigated over the past decade with voltage-jump and concentration-jump relaxations, as well as with fluorescence and flow-quench methods. There are still some uncertainties: the biochemical studies might measure binding to the desensitized rather than to the active state (Heidmann and Changeux, 1979; Boyd and Cohen, 1980; Prinz and Maelicke, 1984), and the electrophysiological studies could be measuring a rate-limiting conformational change rather than a binding (Sheridan and Lester, 1977; Lester et al., 1980; Ogden and Colquhoun, 1983). Nonetheless, there is now general agreement that the agonist-receptor binding proceeds with a forward rate constant of 10^8–10^9 M^{-1} s^{-1} at 20°C, with the bis-quaternary compounds falling in the high end of this range. The present data show that antagonist-receptor binding proceeds with rates about an order of magnitude smaller. The most direct comparisons involve the concentration-jump experiments using the photoisomerizable bis-quaternary azobenzene derivatives. The agonist Bis-Q binds with rates of $\sim 10^9$ M^{-1} s^{-1} at 20°C (Sheridan and Lester, 1977; Lester et al., 1980) vs. the value of 10^8 M^{-1} s^{-1} determined for 2BQ in the present study. These differences in binding rate are probably small enough to agree with the generally held view that (*a*) antagonists and agonists have similar initial steric and coulombic interactions with the receptor's binding site, but (*b*) only the latter allow the subsequent conformational changes that open the channel.

There are exceptions to this pleasing concordance. First, in experiments analogous to that of Fig. 2, *d*-tubocurarine decreased both the steady state activation and the relaxation rate constant for voltage-jump relaxations (Sheridan and Lester, 1977; Colquhoun and Sheridan, 1982). The usual interpretation of the *d*-tubocurarine result is that it equilibrates rapidly with receptors (severalfold

more rapidly than the agonist itself). This admittedly indirect evidence leads to the conclusion that *d*-tubocurarine binds with rates that push the limits of physical possibility. We now think that this apparent anomaly can be explained by a special combination of equilibrium and kinetic properties (Krouse, M. E., and H. A. Lester, manuscript in preparation). Second, the so-called "open channel blockers" seem to bind one or two orders of magnitude more slowly, even when this binding is accelerated by the membrane field (Adams, 1976; Neher and Steinbach, 1978). Presumably, the binding site is different from the one under consideration here—it may be directly within the open channel.

What Are the Rates for trans-2BQ?

In contrast to the consistent picture obtained for *cis*-2BQ, our data do not allow clear conclusions about the kinetics of the interaction between *cis*-2BQ and the receptor. One set of experiments involved component $1_{l\text{-}f}$, the rapid increase observed after *cis* → *trans* photoisomerization of bound 2BQ molecules. To obtain relaxations that were dominated by the dissociation of *trans*-2BQ, it was necessary to employ the most rapidly equilibrating agonist, carbachol, and to use laser flashes (Fig. 9). From these data, one might infer that the interaction between *trans*-2BQ and the receptor proceeds with characteristic times on the order of 1 ms. However, another set of experiments measured the time required for the relaxation back to equilibrium after unfiltered flashes at the *trans*-photostationary state (Fig. 10). From these data, one might infer that hundreds of milliseconds are involved. We suspect that both inferences are misleading and that the actual rates lie between these two extremes. Component $1_{l\text{-}f}$ probably does not directly reflect the lifetime of newly created *trans*-2BQ on the receptor because (*a*) the *trans*-2BQ-receptor complex has received a large amount of energy from the photon and (*b*) the ligand may be bound in a different configuration (or range of configurations) than if it had entered normally from the free solution. Thus, the kinetics of this relaxation may not reflect the same molecular events as the equilibrium studies with *trans*-2BQ.

We have considered two possible mechanisms for the long relaxations of Fig. 10. (*a*) In the *trans*-photostationary solution, the proportion of *trans* is ~80%. Although the *cis* isomer exhibits a threefold-greater binding constant, *trans*-2BQ-receptor complexes are slightly more numerous. The relaxations are thus slowed under those conditions where the *trans*-2BQ-receptor interaction would be expected to dominate the kinetics. To examine this possibility, we extended our kinetic model (Scheme 2) to include *trans*-2BQ-receptor interactions at the same binding sites that bind agonist and *cis*-2BQ. We were at first surprised that the model could not reproduce the observed 3.5-fold slowing, even with the many free parameters offered by nine states and even if the kinetics for the *trans* isomer were 30-fold slower than for the *cis* isomer. We then realized that the decrease in conductance is still dominated by the fastest inhibition, that caused by the *cis* isomer. Thus, the slow relaxations are not explained by a slow *trans*-2BQ-receptor interaction.

(*b*) Buffered diffusion could play a role in the slowing. The unfiltered flashes, with a large *cis* → *trans* flux, markedly deplete the synaptic cleft of *cis*-2BQ, most

of it previously bound to receptors. In order to re-establish equilibrium, *cis*-2BQ must therefore diffuse in from the external solution (steps *e* and *f* in Fig. 11), and this diffusion would be slowed by multiple binding.

Rough calculations suggest that the buffering model can easily account for the slow relaxations. If one begins with the data of Armstrong and Lester (1979, Fig. 8*A*) and corrects for the slightly higher affinity of *cis*-2BQ for the receptor as compared with *d*-tubocurarine, one concludes that a relaxation rate constants as slow as 2 s^{-1} would still be explained by buffered diffusion. The fact that the relaxations were about threefold faster may arise because (*a*) some *cis*-2BQ molecules do remain within the synaptic cleft during the flash and (*b*) buffering is reduced by the agonist-receptor interactions. Thus, we tentatively suggest that the slow relaxations of Fig. 10 reflect buffered diffusion of *cis*-2BQ molecules as they enter the synaptic cleft.

We did not notice the same slowing phenomemon in preliminary experiments at 20°C. However, if this very slow phase has a rather low temperature dependence, its rate would be near that of the noncompetitive channel block effect. Thus, the temperature test could not be cleanly applied to decide whether the slow relaxations are governed by the *trans*-2BQ-receptor interaction or by buffered diffusion of *cis*-2BQ as it re-enters the synaptic cleft.

It would be helpful to have comparable data from a preparation not subject to buffered diffusion. Because cultured myoballs lack synapses and have a low receptor density, buffered diffusion is not expected to play a role in the kinetics of drug action. Light-flash experiments are under way with patch-clamped rat myoballs (Chabala et al., 1982, 1984; Lester and Chabala, 1984).

We thank R. Spencer for assistance in all phases of the project and J. M. Nerbonne, J. Pine, and D. Van Essen for advice.

This research was sponsored by the National Institutes of Health (research grants NS-11756 and NS-15581) and by a grant-in-aid from the Muscular Dystrophy Association of America. M.E.K. was supported in part by predoctoral training grants from the National Institutes of Health (GM-07737) and by the Weigle Memorial Fund.

Original version received 24 September 1984 and accepted version received 29 March 1985.

REFERENCES

Adams, P. R. 1975. An analysis of the dose-response curve at voltage-clamped frog endplates. *Pflügers Arch. Eur. J. Physiol.* 360:145–153.

Adams, P. R. 1976. Drug blockage of open endplate channels. *J. Physiol. (Lond.).* 260:531–552.

Armstrong, D., and H. A. Lester. 1979. The kinetics of curare action and restricted diffusion within the synaptic cleft. *J. Physiol. (Lond.).* 294:365–386.

Blackman, J. G., R. W. Gauldie, and R. Milne. 1975. Interaction of competitive antagonists: the anticurare action of hexamethonium and other antagonists at the skeletal neuromuscular junction. *Br. J. Pharmacol.* 54:91–100.

Boyd, N. D., and J. B. Cohen. 1980. Kinetics of binding of [^{3}H]acetylcholine to *Torpedo* postsynaptic membranes: association and dissociation rate constants by rapid mixing and ultrafiltration. *Biochemistry.* 19:5353–5358.

Chabala, L. D., A. M. Gurney, and H. A. Lester. 1984. patch-clamp studies of ACh channels activated by photoisomerizable agonists. *Biophys. J.* 45:387*a*. (Abstr.)

Chabala, L. D., H. A. Lester, and R. E. Sheridan. 1982. Single-channel currents from cholinergic receptors in cultured muscle. *Soc. Neurosci. Abstr.* 8:498.

Colquhoun, D. C. 1973. The relation between classical and cooperative models for drug action. *In* Drug Receptors. H. P. Rang, editor. MacMillan, London. 149–182.

Colquhoun, D., F. Dreyer, and R. E. Sheridan. 1979. The actions of tubocurarine at the frog neuromuscular junction. *J. Physiol. (Lond.).* 293:247–284.

Colquhoun, D. C., and R. E. Sheridan. 1982. The effect of tubocurarine competition on the kinetics of agonist action on the nicotinic receptor. *Br. J. Pharmacol.* 75:77–86.

del Castillo, J., and B. Katz. 1957. A study of curare action with an electrical micro-method. *Proc. R. Soc. Lond. B Biol. Sci.* 146:339–356.

Heidmann, T., and J. P. Changeux. 1979. Fast kinetic studies on the interaction of a fluorescent agonist with the membrane-bound acetycholine receptor from *Torpedo marmorata*. *Eur. J. Biochem.* 94:225–279.

Hill, A. V. 1909. The mode of action of nicotine and curari, determined by the form of the contraction curve and the method of temperature coefficients. *J. Physiol. (Lond.).* 39:361–373.

Jenkinson, D. H. 1960. The antagonism between tubocurarine and substances which depolarize the motor endplate. *J. Physiol. (Lond.).* 152:309–324.

Krouse, M. E. 1984. Investigation of competitive antagonist binding to the nicotinic acetylcholine receptor using voltage-jump and light-flash techniques. Ph.D. Dissertation. California Institute of Technology, Pasadena, CA. University Microfilms, Ann Arbor, MI. 100 pp.

Krouse, M. E., H. A. Lester, B. F. Erlanger, and N. H. Wassermann. 1982. A study of the nicotinic acetylcholine receptor using a photoisomerizable competitive antagonist. *Soc. Neurosci. Abstr.* 8:498.

Krouse, M. E., H. A. Lester, B. F. Erlanger, and N. H. Wassermann. 1984. The measurement of the rate constants for a competitive antagonist of the nicotinic acetylcholine receptor. *Biophys. J.* 45:387*a*. (Abstr.)

Lester, H. A., and L. D. Chabala. 1984. Neither monoliganded nor desensitized receptors account for excess brief acetylcholine channels in cultured rat muscle. *Neurosci. Abstr.* 10:12.

Lester, H. A., and H. W. Chang. 1977. Response of acetylcholine receptors to rapid, photochemically produced increases in agonist concentration. *Nature (Lond.).* 266:373–374.

Lester, H. A., J.-P. Changeux, and R. E. Sheridan. 1975. Conductance increases produced by bath application of cholinergic agonists to *Electrophorus* electroplaques. *J. Gen. Physiol.* 65:797–816.

Lester, H. A., and J. M. Nerbonne. 1982. Physiological and pharmacological manipulations with light flashes. *Annu. Rev. Biophys. Bioeng.* 11:151–175.

Lester, H. A., D. D. Koblin, and R. E. Sheridan. 1978. Role of voltage-sensitive receptors in nicotinic transmission. *Biophys. J.* 21:181–194.

Lester, H. A., M. E. Krouse, M. M. Nass, N. H. Wassermann, and B. F. Erlanger. 1979. Light-activated drug confirms a mechanism of ion channel blockade. *Nature (Lond.).* 280:509–510.

Lester, H. A., M. E. Krouse, M. M. Nass, N. H. Wassermann, and B. F. Erlanger. 1980. A covalently bound photoisomerizable agonist. Comparison with reversibly bound agonists at *Electrophorus* electroplaques. *J. Gen. Physiol.* 75:207–232.

Manalis, R. S. 1977. Voltage-dependent effect of curare at frog neuromuscular junction. *Nature (Lond.).* 267:366–368.

Morris, C. E., B. S. Wong, M. B. Jackson, and H. Lecar. 1983. Single-channel currents activated by curare in cultured embryonic rat muscle. *J. Neurosci.* 3:2525–2531.

Nargeot, J., H. A. Lester, N. J. M. Birdsall, J. Stockton, N. H. Wassermann, and B. F. Erlanger. 1982. A photoisomerizable muscarinic antagonist. Studies of binding and of conductance relaxations in frog heart. *J. Gen. Physiol.* 79:657–678.

Nass, M. M., H. A. Lester, and M. E. Krouse. 1978. Response of acetylcholine receptors to photoisomerizations of bound agonist molecules. *Biophys. J.* 24:135–160.

Neher, E., and B. Sakmann. 1975. Voltage-dependence of drug-induced conductance in frog neuromuscular junction. *Proc. Natl. Acad. Sci. USA.* 72:2140–2144.

Neher, E., and J. H. Steinbach. 1978. Local anaesthetics transiently block currents through single acetylcholine-receptor channels. *J. Physiol. (Lond.).* 277:153–176.

Nerbonne, J. M., R. E. Sheridan, L. D. Chabala, and H. A. Lester. 1983. *Cis*-Bis-Q: purification and properties at acetylcholine receptors of *Electrophorus* electroplaques. *Mol. Pharmacol.* 23:344–349.

Neubig, R. R., and J. B. Cohen. 1979. Equilibrium binding of [^{3}H]tubocurarine and [^{3}H]-acetylcholine by *Torpedo* postsynaptic membranes: stoichiometry and ligand interactions. *Biochemistry.* 18:5464–5475.

Ogden, D. C., and D. Colquhoun. 1983. The efficacy of agonists at the frog neuromuscular junction studied with single channel recording. *Pflügers Arch. Eur. J. Physiol.* 399:246–248.

Pennefather, P., and D. M. J. Quastel. 1981. Relationship between subsynaptic receptor blockade and response to quantal transmitter at the mouse neuromuscular junction. *J. Gen. Physiol.* 78:313–344.

Prinz, H., and A. Maelicke. 1984. Interaction of cholinergic ligands with the purified acetylcholine receptor protein. II. Kinetic studies. *J. Biol. Chem.* 258:10273–10282.

Sheridan, R. E., and H. A. Lester. 1975. Relaxation measurements on the acetylcholine receptor. *Proc. Natl. Acad. Sci. USA.* 72:3496–3500.

Sheridan, R. E., and H. A. Lester. 1977. Rates and equilibria at the acetylcholine receptor of *Electrophorus* electroplaques. A study of neurally evoked postsynaptic currents and of voltage-jump relaxations. *J. Gen. Physiol.* 70:187–219.

Sheridan, R. E., and H. A. Lester. 1982. Functional stoichiometry at the nicotinic receptor. The photon cross-section for phase 1 corresponds to two Bis-Q molecules per channel. *J. Gen. Physiol.* 80:499–515.

Sine, S. M., and P. Taylor. 1981. Relationship between antagonist occupancy and the functional capacity of the acetylcholine receptor. *J. Biol. Chem.* 256:6692–6699.

Trautmann, A. 1982. Curare can open and block ionic channels associated with cholinergic receptor. *Nature (Lond.).* 298:272–275.

Wassermann, N. H., and B. F. Erlanger. 1981. Agents related to a potent activator of the acetylcholine receptor of *Electrophorus* electroplaques. *Chem-Biol. Interact.* 36:251–258.